Microscopic Description of the Granular Fluidity Field in Nonlocal Flow Modeling

Qiong Zhang and Ken Kamrin*
Department of Mechanical Engineering, MIT, Cambridge, Massachusetts 02139, USA
(Received 22 June 2016; revised manuscript received 9 November 2016; published 31 January 2017)

A recent granular rheology based on an implicit "granular fluidity" field has been shown to quantitatively predict many nonlocal phenomena. However, the physical nature of the field has not been identified. Here, the granular fluidity is found to be a kinematic variable given by the velocity fluctuation and packing fraction. This is verified with many discrete element simulations, which show that the operational fluidity definition, solutions of the fluidity model, and the proposed microscopic formula all agree. Kinetic theoretical and Eyring-like explanations shed insight into the obtained form.

DOI: 10.1103/PhysRevLett.118.058001

The rheology of dry granular materials is commonly studied in homogeneous simple (planar) shear tests. In these tests, the *inertial granular rheology* can be observed, in which a one-to-one relationship exists between two dimensionless numbers: $\mu = \tau/P$, the ratio of shear stress τ to normal stress P, and the inertial number $I = \dot{\gamma} d/\sqrt{P/\rho_s}$, which nondimensionalizes the shear rate $\dot{\gamma}$ by the (mean) particle size d, P, and the solid density ρ_s [1,2]. Empirically, the bijection between μ and I is often fitted to the form [3]

$$\mu = \mu_{\mathrm{loc}}(I) = \mu_s + \frac{\Delta\mu}{I_0/I + 1}, \tag{1}$$

where μ_s is a static yield coefficient, below which the system does not flow, μ_2 is an upper limit for μ at high rates, $\Delta\mu = \mu_2 - \mu_s$, and I_0 is a dimensionless constant. Despite its effectiveness in steady simple shearing, granular behavior in more general circumstances can be observed to deviate from the inertial rheology. In inclined plane flows, where the μ field is spatially homogeneous and given by the tilt angle, the angle at which a flowing layer stops depends explicitly on the size (thickness) of the pile [4,5]. In steady but nonuniform flow geometries, flow is observed in zones where $\mu < \mu_s$, and the $\mu(I)$ relation is not one to one in these regions [6,7]. Moreover, a "secondary rheology" has been observed in which the dynamics of a loaded probe submerged in quiescent material is influenced by the motion of faraway boundaries of the granular system [8,9]. Such phenomena deviating from the inertial law are describable by considering nonlocal effects. Various microscopic notions have been considered for the intrinsic length scale [10–15].

Recently, a size-dependent granular rheological framework was proposed based on a state field called the "granular fluidity." With minimal fitting parameters, the model has shown the capability of quantitatively predicting a range of nonlocal effects in multiple geometries, including all of the deviations from $\mu(I)$ behavior described above [16–21]. The granular fluidity field, denoted g, is presumed to be governed by a dynamical partial differential equation (PDE) [21]:

$$t_0\dot{g} = A^2 d^2 \nabla^2 g - \Delta\mu\left(\frac{\mu_s - \mu}{\mu_2 - \mu}\right) g - b\sqrt{\frac{\rho_s d^2}{P}}\mu g^2, \tag{2}$$

where A is a dimensionless constant called the *nonlocal amplitude*, t_0 is a time scale, and $b = \Delta\mu/I_0$ [22]. The g field influences the flow through its role in the constitutive relation between the stress and the strain rate: $\dot{\gamma} = g\mu$. Together, the result is a flow model with an intrinsic length scale given by d. The inertial law, Eq. (1), can be obtained when the flow field is homogeneous ($\nabla g = \vec{0}$) and in steady state. While these equations define the model from a mathematical perspective, the physical nature of the granular fluidity field is not clear. To be valid in its role within the constitutive model, granular fluidity should be a kinematically observable state variable. However, it is not clear this is the case, and it has been suggested g may not represent a kinematic field [23]. We are left to ask the following: What *is* the granular fluidity?

In this Letter, we identify a microphysical definition for the granular fluidity. While many microscopic variables have been proposed to underpin grain-size-dependent flow models—including stress fluctuations [24], plastic strain-rate variations [25], granular eddies [26,27], the fraction of sliding contacts [28,29], or spots of free volume [30]—we find the granular fluidity is well defined solely in terms of velocity fluctuations and the packing fraction. Using discrete element method (DEM) simulations in multiple configurations at steady state, we compare the predictions of this microscopic formula with the constitutive definition $g = \dot{\gamma}/\mu$, as well as steady solutions of g from the PDE for granular fluidity. The strong agreement found gives evidence that the PDE is in fact a model for the behavior of this kinematic field. Lastly, we identify two possible reasons for the microscopic description of g, using kinetic theory and also using an Eyring-like model, which illustrates a possible fluctuation activated process of granular flows.

 © 2017 American Physical Society

We start with the hypothesis that, for hard particles, g should relate to velocity fluctuations, δv, a quantity key to a number of granular flow models [8,31–35]. From its constitutive definition, $g = \dot{\gamma}/\mu$ has dimensions of inverse time. We propose that the relevant time scale is $d/\delta v$, such that the fluidity g can be nondimensionalized as $gd/\delta v$. Supposing that the only other variable affecting g is the packing fraction, Φ, the normalized fluidity would be expressible as

$$\frac{gd}{\delta v} = F(\Phi) \Rightarrow g = \frac{\delta v}{d} F(\Phi) \tag{3}$$

for some function F.

To evaluate the hypothesis, DEM simulations of three kinds of configurations were implemented in the open-source software LAMMPS [36]. The particles simulated were spheres with a solid density $\rho_s = 2500\ \mathrm{kg/m^3}$, a mean diameter $d = 0.0008$ m, and a polydispersity of 20% to prevent crystallization. The particle interaction model [7,18] contains elastic forces, damping effects, and Coulomb friction using a spring-dashpot law defined by stiffness in the normal and tangential directions k_n, $k_t = 2/7k_n$, damping in the normal and tangential directions γ_n, γ_t, and a surface friction coefficient $\mu_c = 0.4$. We set $\gamma_t = 0$ and calculate γ_n to give a restitution coefficient of $e = 0.1$: $\gamma_n = -2\ln e\sqrt{mk_n/(\pi^2 + \ln^2 e)}$. Throughout, $k_n/Pd > 10^4$ is kept, which ensures that the deformation of the particles is small enough to be in the hard particle regime. The simulated system is a cuboid domain [$8 \times 20 \times \sim 50$ ($x \times y \times z$), 9096 particles in total] of particles shearing between two planar rough walls made of particles of the same properties at the top and bottom. The bottom wall is fixed in all cases. If a pressure boundary condition at the top wall is needed, the top wall's height is controlled to set the pressure using a feedback process [7]. To apply a fixed volume boundary condition, the top wall is held at a fixed z. Periodic boundary conditions are applied to the other four boundaries.

When a steady state is reached, we output data every 20 000 steps, collecting a total of $N = 3000$ snapshots for each simulation. We used three families of configurations: homogeneous planar shear, planar shear with gravity, and chute flows, as shown in Fig. 1. The confining pressure at the top boundary is $P_{\mathrm{wall}} = P_f P_0$, where $P_0 = 5 \times 10^{-6} k_n/d$, the gravity is $G = G_f g_0$, where $g_0 = 0.1 P_0 d^2/m$, and the horizontal velocity of the top wall is $V_{\mathrm{wall}} = V_f\sqrt{6P_0/\pi\rho_s}$, where P_f, G_f, and V_f are dimensionless factors for controlling the boundary conditions and the gravity. In gravity-free planar shear cases, the confining pressure is chosen as $P_f = 1$ and ten different V_f's are used. In planar shear with gravity tests, G_f is fixed at $G_f = 1$ and five cases are simulated with four different V_f's and two P_f's. In chute flow cases, inclination angles of $\theta = 90°$, 75°, 60°, and 45° are simulated. Gravity is increased to $G_f = 3$ in the slanted configurations, and the top wall is fixed in the x direction, $V_f = 0$. We test fixed volume top-wall constraints for all chute cases. We also perform fixed top-wall pressure constraints in the $\theta = 90°$ chute case, where, to make a direct comparison, the confining pressure is chosen to be the same as the mean pressure at the top wall in the corresponding fixed volume case. In total, 20 different flows are simulated.

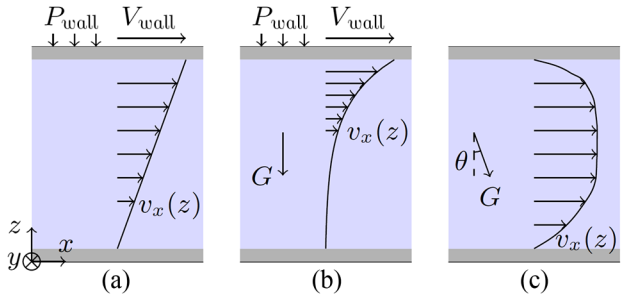

FIG. 1. Configurations of granular flow geometries tested, with qualitative velocity profiles plotted. (a) Planar shear. (b) Planar shear with gravity. (c) Chute flows. Chute flow cases with a fixed top-wall pressure are also performed.

In all geometries, the time-averaged fields should be homogeneous in each horizontal (x-y) plane. For each snapshot, we first produce coarse-grained fields in z using a slab-shaped coarse-graining region, comprising the whole horizontal expanse (x-y planes) and a z thickness of $W = 2d$. We then average these instantaneous layerwise values arithmetically in time. To compute δv at each snapshot, the layerwise-averaged instantaneous velocity is first calculated. We then subtract it from the particle velocities to obtain the velocity deviation. The velocity fluctuation δv is defined as the root of *granular temperature*, which is the mean square of the velocity deviation. For our purposes, it is key that δv be defined this way, based on deviations from an instantaneous average of the velocity; definitions that compute deviations from a time-averaged velocity are common but inappropriate here (and do not collapse the data) because they pick up time oscillations in otherwise rigid collections of grains rather than measuring only the relative motion of grains. The particlewise stress tensor is calculated considering both the contact contribution and the kinetic contribution, as defined in Ref. [7], though the contact contribution is 2 orders larger than the kinetic almost everywhere in our tests. After the average Cauchy stress tensor has been obtained in a layer, the pressure is defined as $P = -\sigma_{ii}/3$ and the shear stress is defined as the equivalent shear stress, $\tau = \sqrt{\sigma'_{ij}\sigma'_{ij}/2}$, where $\sigma'_{ij} = \sigma_{ij} + P\delta_{ij}$ is the stress deviator. See the Supplemental Material [37] for details of the averaging method and its verification.

To be free of wall effects, we have excluded layers within $2d$ of the walls. To ensure steady-state conditions, we accept data from layers that have experienced a strain no

smaller than 25 in sampling. See the Supplemental Material [37] for more discussion on the selection of these criteria. The span of inertial numbers in the data presented is 0.000 6 to 0.7, which covers the range from quasistatic to collisional flow [2].

To evaluate if $g = F(\Phi)\delta v/d$, we calculate the layerwise fluidity field $g = \dot{\gamma}/\mu$, δv, and Φ in all cases. For added precision, here we evaluate d as the layerwise mean particle size; though quasimonodisperse, the packing shows slight ($\lesssim$10%) spatial variation in d. We plot the normalized fluidity $gd/\delta v$ against the packing fraction Φ in Fig. 2 for all 20 flows simulated. Each data point corresponds to a different z value, except gravity-free planar shear cases, which are nearly uniform and show a single data point per test. The data from different configurations collapse well, suggesting that packing fraction and velocity fluctuations are sufficient to define the granular fluidity. $F(\Phi)$ has a nearly constant behavior for low Φ values, which transitions into a roughly linear decrease at high values. This behavior can be fit to a hyperbola $F(\Phi) = [-(\Phi - 0.58) + \sqrt{(\Phi - 0.58)^2 + 1.54 \times 10^{-4}}]/0.048 + 2.0$, which vanishes at $\Phi = 0.63$, approximately random close packing. This fit line provides a good match to our data, though we were only able to obtain accurate steady-state data up to $\Phi \approx 0.62$. Finite values of g above 0.63 may be possible. An interpretation for the collapse of the data and the corresponding shape of $F(\Phi)$ will be given later.

For further examination, in Fig. 3 the predicted fluidity fields from the microscopic formula [using the above fit for $F(\Phi)$] are compared with $\dot{\gamma}/\mu$ and solutions of Eq. (2) in all configurations tested. In the PDE, $b = 0.98$, $\mu_s = 0.37$, and $\mu_2 = 0.95$ are obtained by fitting the $\mu(I)$ relation in the homogeneous planar shear cases as shown in Fig. 3(a), and we choose $A = 0.43$. All of these values are close to the values found for glass spherical beads [3,17], with the exception of μ_2, which we find to be larger in our discrete simulations [47]. The boundary condition for g is taken as the wall value of $\dot{\gamma}/\mu$ from the DEM, and the PDE is run to steady state using a finite-difference method to obtain steady g profiles. Note that the fluidity profiles of 90° chute flow cases with fixed volume boundary conditions and fixed pressure boundary conditions match well, as compared in Fig. 3(c), showing that the type of boundary condition does not have a significant influence on the constitutive behavior in the interior. This is also the case if the incline angle is varied, which we verified in additional tests. Overall, the agreement of the three descriptions of the g field in all geometries evidences the generality of the $g = F(\Phi)\delta v/d$ formula and its apparent connection to the steady solutions of Eq. (2).

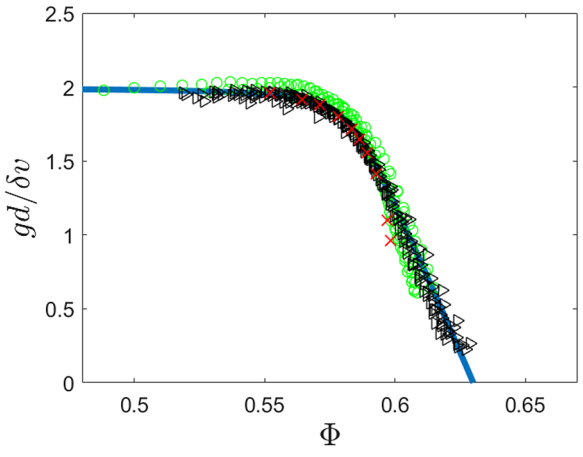

FIG. 2. Data from all chute flow tests (right-pointing triangles), planar shear with gravity tests (circles), and homogeneous planar shear tests (crosses). A hyperbola (the solid line) is fit for $F(\Phi)$.

In an attempt to explain the fluidity formula, we have found two possible routes, one using kinetic theory and another based on activated processes. Regarding kinetic theory, in Lun *et al.*'s work [48], P and the viscosity η in a granular gas depend on Φ and the granular temperature T:

$$P(\Phi, T) = \rho F_1(\Phi) T \quad \text{and} \quad \eta(\Phi, T) = \rho d F_2(\Phi)\sqrt{T}, \tag{4}$$

where ρ is the density. Under these relations, the operational definition of fluidity would imply

$$g = \frac{\dot{\gamma}}{\mu} = \frac{P}{\eta} = \frac{\rho F_1(\Phi) T}{\rho d F_2(\Phi)\sqrt{T}} = \frac{\sqrt{T}}{d}\frac{F_1(\Phi)}{F_2(\Phi)} = \frac{\delta v}{d}\frac{F_1(\Phi)}{F_2(\Phi)},$$

whose form is the same as Eq. (3). Though the fitted $F(\Phi)$ is different from $F_1(\Phi)/F_2(\Phi)$ as given in Ref. [48], the similarity of the form is suggestive. Since nonlocal effects are most evident in quasistatic regions, an extended kinetic theory [49] might be needed to further this connection, where behavior beyond binary collisions is modeled. That said, there is evidence in dense annular shear experiments [50] of a density- and temperature-dependent granular viscosity consistent with the above form.

Even though our formula for g agrees with the functional scaling from kinetic theory, we find, contrary to the kinetic theoretical picture, that the individual forms for pressure and viscosity [Eq. (4)] are actually not well satisfied in our data beyond $\Phi = 0.57$; see the Supplemental Material [37] for additional data comparisons and more discussion relating to the models in Refs. [48,50,51]. The pressure may collapse better if permitted to depend on additional fields, like gradients of strain rate, or on particle properties such as stiffness [52]. Since Eq. (2) evolves g as a single state variable, it is natural to ask if the observed relation $g(\delta v, \Phi)$ can be reduced to depend on only one state variable rather than two. Perhaps the pressure could be used to eliminate Φ or δv from the system. However, without a clear equation relating P to Φ and δv in dense zones, such a reduction looks unlikely.

Eyring's model [53] for activated processes has an analogy in the flow behavior of glassy solids [54].

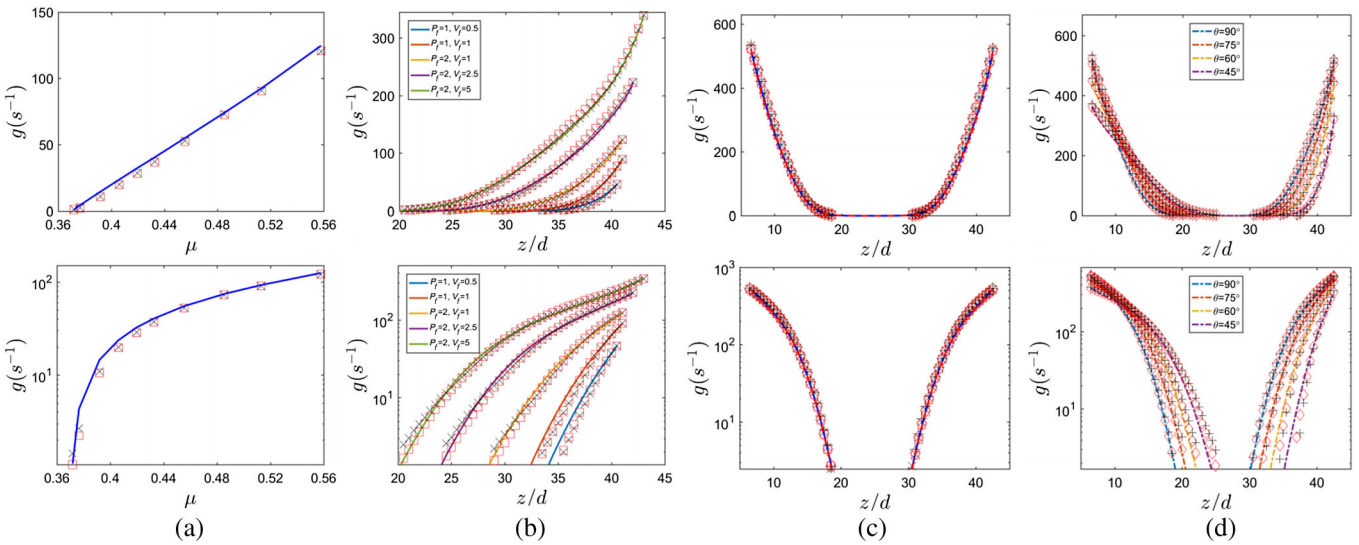

FIG. 3. Comparison of three definitions of g: DEM results of $\dot{\gamma}/\mu$ (square, diamond), solutions of Eq. (2) (the lines), and predictions of the microscopic formula, Eq. (3) (cross, plus). Comparisons in (a) homogeneous planar shear cases, (b) planar shear with gravity, (c) 90° chute flow cases with different boundary conditions, and (d) chute flow cases at different inclinations. Results of DEM simulations using fixed volume boundary conditions (BCs) are indicated by (diamond, plus) and fixed wall pressure BCs by (square, cross).

Similar ideas have also been considered in the context of granular flows [8,24]. We propose the following Eyring-like micromodel. Suppose a material element contains a collection of microscopic "sites," each able to undergo a shear event or "hop." We express the element's total shear rate through the product

$$\dot{\gamma} = \begin{pmatrix} \text{Fraction} \\ \text{of sites} \\ \text{able to} \\ \text{shear} \end{pmatrix} \begin{pmatrix} \text{Net no. of} \\ \text{forward shear} \\ \text{events per site} \\ \text{per second} \end{pmatrix} \begin{pmatrix} \text{Strain} \\ \text{per} \\ \text{shear} \\ \text{event} \end{pmatrix}. \quad (5)$$

We assume [54] that the fraction of sites with enough local free volume to support a shear event is some function of the coarse-grained packing fraction, $f_1(\Phi)$. It may approach 0 at a jammed Φ value, ≈63%. The second term can be expressed as the product of an attempt frequency for perturbations, ω, and the net probability, $\mathrm{Pr}^+ - \mathrm{Pr}^-$, that a perturbation causes a positive shear event vs a backward (negative) event on a site. The frequency of attempts should be related to the fluctuational motion of the particles, so we assume ω is given by $\delta v f_2(\Phi)/d$, i.e., the ratio of velocity fluctuation to a characteristic fluctuation length $d/f_2(\Phi)$. For the net probability, $\mathrm{Pr}^+ - \mathrm{Pr}^-$ is 0 by symmetry when there is no external shear loading, and otherwise should grow with the loading. Hence, the linearized dependence on μ should follow $\mathrm{Pr}^+ - \mathrm{Pr}^- = f_3(\Phi)\mu$. Because the ratio $\rho\delta v^2/P$ is smaller than 0.01 almost everywhere, the kinetic energy of the fluctuations is too small to assist flow events, which is why we have assumed, as others have [24], that the net probability is independent of δv (see the Supplemental Material [37] for additional details about the form of $\mathrm{Pr}^+ - \mathrm{Pr}^-$). Lastly, we make the common assumption [24,54,55] that the strain per flow event is a constant, γ_0, related to a typical "jump distance" normalized by the width of a shear event. We now multiply the three factors together to get $\dot{\gamma} = \gamma_0 \delta v f_1(\Phi) f_2(\Phi) f_3(\Phi)\mu/d$. Dividing by μ, one obtains

$$g = \frac{\dot{\gamma}}{\mu} = \frac{\delta v}{d} \underbrace{\gamma_0 f_1(\Phi) f_2(\Phi) f_3(\Phi)}_{F(\Phi)}. \quad (6)$$

Since γ_0 is constant, Eq. (6) has the same form as Eq. (3). This analysis suggests that shear flow in granular media may be a fluctuation activated process.

Supposing that f_1 is the dominant contribution to F, Fig. 2 suggests a natural interpretation. When $\Phi < 0.57$, the packing is open enough that all sites are able to flow, and f_1 holds at its maximum. As the packing fraction increases above 0.57, the number of sites with enough free volume for flow gradually decreases. The Cohen-Turnbull theory of free-volume distribution in glassy materials gives a similar behavior for the fraction of sites above a critical free-volume threshold [56].

Herein, we have proposed a relation connecting granular fluidity to granular velocity fluctuations and packing fraction, and we have validated it in DEM simulations of multiple configurations. All three descriptions of the granular fluidity field—(i) its operational definition ($g = \dot{\gamma}/\mu$) extracted from DEM simulations, (ii) its definition from the fluidity governing PDE, and (iii) the new microphysical definition—match well with each other in multiple geometries under multiple conditions. It is also interesting to compare the description herein to related nonlocal models for nongranular materials (e.g. emulsions

and suspensions), which deal with the "standard" fluidity $f = \dot{\gamma}/\tau$ (the inverse viscosity) [57,58] rather than g. Theories have previously suggested that f relates microscopically to the rate of plastic events [58], which has been correlated to shear-rate variations in experiments [25]. Although the variables are different, the fact that fluctuation in a certain variable is key to both pictures suggests a bridge between the different amorphous material classes. Deriving Eq. (2) from the microscopic description of g remains crucial future work. Under kinetic theory assumptions, Eq. (2) might relate to a heat equation. We should also point out that the above tests only used one combination of restitution coefficient and surface friction coefficient; the function $F(\Phi)$ need not stay the same as these inputs are varied. Lastly, though we have found two state variables sufficient to describe granular fluidity, other fields such as higher moments of velocity fluctuation or fabric invariants [59] may provide additional improvements.

Q. Z. and K. K. acknowledge support from National Science Foundation Grant No. CBET-1253228 and the MIT Department of Mechanical Engineering.

*kkamrin@mit.edu

[1] B. Andreotti, Y. Forterre, and O. Pouliquen, *Granular Media: Between Fluid and Solid* (Cambridge University Press, Cambridge, 2013).
[2] F. da Cruz, S. Emam, M. Prochnow, J.-N. Roux, and F. Chevoir, Phys. Rev. E **72**, 021309 (2005).
[3] P. Jop, Y. Forterre, and O. Pouliquen, J. Fluid Mech. **541**, 167 (2005).
[4] L. E. Silbert, J. W. Landry, and G. S. Grest, Phys. Fluids **15**, 1 (2003).
[5] G. MiDi, Eur. Phys. J. E **14**, 341 (2004).
[6] F. Da Cruz, F. Chevoir, D. Bonn, and P. Coussot, Phys. Rev. E **66**, 051305 (2002).
[7] G. Koval, J.-N. Roux, A. Corfdir, and F. Chevoir, Phys. Rev. E **79**, 021306 (2009).
[8] K. A. Reddy, Y. Forterre, and O. Pouliquen, Phys. Rev. Lett. **106**, 108301 (2011).
[9] K. Nichol, A. Zanin, R. Bastien, E. Wandersman, and M. van Hecke, Phys. Rev. Lett. **104**, 078302 (2010).
[10] F. Radjai and S. Roux, Phys. Rev. Lett. **89**, 064302 (2002).
[11] O. Pouliquen, Phys. Rev. Lett. **93**, 248001 (2004).
[12] G. Lois, A. Lemaitre, and J. Carlson, Europhys. Lett. **76**, 318 (2006).
[13] L. Staron, Phys. Rev. E **77**, 051304 (2008).
[14] L. Staron, P.-Y. Lagrée, C. Josserand, and D. Lhuillier, Phys. Fluids **22**, 113303 (2010).
[15] M. Bouzid, M. Trulsson, P. Claudin, E. Clément, and B. Andreotti, Phys. Rev. Lett. **111**, 238301 (2013).
[16] K. Kamrin and G. Koval, Phys. Rev. Lett. **108**, 178301 (2012).
[17] D. L. Henann and K. Kamrin, Proc. Natl. Acad. Sci. U.S.A. **110**, 6730 (2013).
[18] K. Kamrin and G. Koval, Comp. Part. Mech. **1**, 169 (2014).
[19] D. L. Henann and K. Kamrin, Int. J. Plast. **60**, 145 (2014).
[20] D. L. Henann and K. Kamrin, Phys. Rev. Lett. **113**, 178001 (2014).
[21] K. Kamrin and D. L. Henann, Soft Matter **11**, 179 (2015).
[22] This is the full form of the granular fluidity relation; an approximation for steady-state solutions only is also commonly used [16,17].
[23] M. Bouzid, A. Izzet, M. Trulsson, E. Clément, P. Claudin, and B. Andreotti, Eur. Phys. J. E **38**, 125 (2015).
[24] O. Pouliquen and Y. Forterre, Phil. Trans. R. Soc. A **367**, 5091 (2009).
[25] P. Jop, V. Mansard, P. Chaudhuri, L. Bocquet, and A. Colin, Phys. Rev. Lett. **108**, 148301 (2012).
[26] T. Miller, P. Rognon, B. Metzger, and I. Einav, Phys. Rev. Lett. **111**, 058002 (2013).
[27] D. Ertaş and T. C. Halsey, Europhys. Lett. **60**, 931 (2002).
[28] D. Volfson, L. S. Tsimring, and I. S. Aranson, Phys. Rev. Lett. **90**, 254301 (2003).
[29] L. Staron, F. Radjai, and J.-P. Vilotte, J. Stat. Mech. (2006) P07014.
[30] M. Z. Bazant, Mech. Mater. **38**, 717 (2006).
[31] L. Bocquet, W. Losert, D. Schalk, T. C. Lubensky, and J. P. Gollub, Phys. Rev. E **65**, 011307 (2001).
[32] Y. Forterre and O. Pouliquen, Phys. Rev. Lett. **86**, 5886 (2001).
[33] B. Utter and R. P. Behringer, Phys. Rev. Lett. **100**, 208302 (2008).
[34] R. Artoni and P. Richard, Phys. Rev. Lett. **115**, 158001 (2015).
[35] J. Gaume, G. Chambon, and M. Naaim, Phys. Rev. E **84**, 051304 (2011).
[36] S. Plimpton, J. Comput. Phys. **117**, 1 (1995).
[37] See Supplemental Material at http://link.aps.org/supplemental/10.1103/PhysRevLett.118.058001, which includes Refs. [38–46], for more details of the averaging methodology, verifications of the averaging method, the strain criterion, the wall effects, detailed comparisons with kinetic theory, supporting information for the Eyring-like explanation, and further discussion of whether $g = g(\delta v, \Phi)$ can be reduced.
[38] T. Weinhart, R. Hartkamp, A. R. Thornton, and S. Luding, Phys. Fluids **25**, 070605 (2013).
[39] R. Artoni and P. Richard, Phys. Rev. E **91**, 032202 (2015).
[40] J. S. Van Zon and F. C. MacKintosh, Phys. Rev. E **72**, 051301 (2005).
[41] J. S. Van Zon and F. C. MacKintosh, Phys. Rev. Lett. **93**, 038001 (2004).
[42] F. Rouyer and N. Menon, Phys. Rev. Lett. **85**, 3676 (2000).
[43] W. Losert, D. Cooper, J. Delour, A. Kudrolli, and J. Gollub, Chaos **9**, 682 (1999).
[44] S. Henkes and B. Chakraborty, Phys. Rev. E **79**, 061301 (2009).
[45] Y. Wu and S. Teitel, Phys. Rev. E **92**, 022207 (2015).
[46] F. Radjai, S. Roux, and J. J. Moreau, Chaos **9**, 544 (1999).
[47] The value of t_0 is irrelevant here, as we study only the steady state.
[48] C. Lun, S. Savage, D. Jeffrey, and N. Chepurniy, J. Fluid Mech. **140**, 223 (1984).
[49] J. T. Jenkins and D. Berzi, Granular Matter **12**, 151 (2010).
[50] W. Losert, L. Bocquet, T. C. Lubensky, and J. P. Gollub, Phys. Rev. Lett. **85**, 1428 (2000).

[51] P. Haff, J. Fluid Mech. **134**, 401 (1983).
[52] D. Berzi and J. T. Jenkins, Soft Matter **11**, 4799 (2015).
[53] H. Eyring, J. Chem. Phys. **4**, 283 (1936).
[54] F. Spaepen, Acta Metall. **25**, 407 (1977).
[55] K. Kamrin and E. Bouchbinder, J. Mech. Phys. Solids **73**, 269 (2014).
[56] M. H. Cohen and D. Turnbull, J. Chem. Phys. **31**, 1164 (1959).
[57] J. Goyon, A. Colin, G. Ovarlez, A. Ajdari, and L. Bocquet, Nature (London) **454**, 84 (2008).
[58] L. Bocquet, A. Colin, and A. Ajdari, Phys. Rev. Lett. **103**, 036001 (2009).
[59] E. Azéma, F. Radjai, and G. Saussine, Mech. Mater. **41**, 729 (2009).